Measurement of the Entropy and Critical Temperature of a Strongly Interacting Fermi Gas

L. Luo, B. Clancy, J. Joseph, J. Kinast, and J. E. Thomas*

Department of Physics, Duke University, Durham, North Carolina 27708, USA

(Received 28 December 2006; published 21 February 2007)

We report a model-independent measurement of the entropy, energy, and critical temperature of a degenerate, strongly interacting Fermi gas of atoms. The total energy is determined from the mean square cloud size in the strongly interacting regime, where the gas exhibits universal behavior. The entropy is measured by sweeping a bias magnetic field to adiabatically tune the gas from the strongly interacting regime to a weakly interacting regime, where the entropy is known from the cloud size after the sweep. The dependence of the entropy on the total energy quantitatively tests predictions of the finite-temperature thermodynamics.

DOI: 10.1103/PhysRevLett.98.080402 PACS numbers: 03.75.Ss, 32.80.Pj

The thermodynamics of strongly interacting Fermi gases is of great interest, as these systems exhibit universal behavior, where the properties are independent of the details of the microscopic interactions [1–4]. These gases provide models for testing nonperturbative many-body theories in a variety of fields from neutron stars and nuclear matter to quark-gluon plasmas and high temperature superconductors. In studies of universal Fermi gases, where thermometry is difficult [5,6], entropy measurement plays a central and fundamental role.

In this Letter, we report the measurement of the entropy S of a strongly interacting Fermi gas as a function of its total energy E. The results yield the temperature T via the elementary thermodynamic relation $1/T = \partial S/\partial E$. Our experiments quantitatively test recent predictions of the entropy based on microscopic many-body theory, yield the dependence of the energy on temperature, and determine the critical temperature for the superfluid transition without invoking any specific theoretical model.

Strongly attractive Fermi gases exhibit both fermionic and bosonic features, and have been studied intensely for several years in experiment [1,7–12] and theory [13–16]. Measurements of the heat capacity [5] and collective mode damping versus energy [17] reveal transitions in behavior, which have been interpreted as a superfluid transition in this system [5]. Recently, the observation of vortices [18] has provided a definitive proof of a superfluid phase. However, there have been no model-independent studies of the thermodynamic properties.

A strongly interacting Fermi gas is prepared using a 50:50 mixture of the two lowest hyperfine states of ^{6}Li atoms in an ultrastable CO_2 laser trap with a bias magnetic field of 840 G, just above a broad Feshbach resonance at $B = 834$ G [19]. At 840 G, the gas is cooled to quantum degeneracy by lowering the trap depth U [1]. Then U is recompressed to $U_0/k_B = 10\ \mu$K, which is large compared to the energy per particle of the gas.

At the final trap depth, U_0, the measured trap oscillation frequencies in the transverse directions are $\omega_x = 2\pi \times 665(2)$ Hz and $\omega_y = 2\pi \times 764(2)$ Hz, while the axial frequency is $\omega_z = 2\pi \times 30.1(0.1)$ Hz at 840 G and $\omega_z = 2\pi \times 33.2(0.1)$ Hz at 1200 G. Note that axial frequencies differ due to the small change in the trapping potential arising from the bias magnetic field curvature. The total number of atoms $N \simeq 1.3(0.2) \times 10^5$ is obtained from absorption images of the cloud using a two-level optical transition at 840 G. The corresponding Fermi energy E_F and Fermi temperature T_F for an ideal (noninteracting) harmonically trapped gas at the trap center are $E_F = k_B T_F \equiv \hbar\bar{\omega}(3N)^{1/3}$, where $\bar{\omega} = (\omega_x\omega_y\omega_z)^{1/3}$. For our trap conditions, we obtain $T_F \simeq 1.0\ \mu$K.

The total energy per particle, E_{840}, of the strongly interacting gas at 840 G is measured in a model-independent way from the mean square size in the axial direction $\langle z^2\rangle_{840}$ [4]. In this strongly interacting regime, the zero energy s-wave scattering length a_S is large compared to the interparticle spacing, which is large compared to the range of the two-body interaction, so that the gas is universal [1–3]. Then, the local pressure is $P = 2\mathcal{E}/3$, where $\mathcal{E}$ is the local energy density [3,4]. Using force balance for a trapping potential U, $\nabla P + n\nabla U = 0$, where n is the local density, one obtains the total energy per particle $E_{840} = 3m\omega_z^2\langle z^2\rangle_{840}(1-\kappa)$ or

$$\frac{E_{840}}{E_F} = \frac{\langle z^2\rangle_{840}}{z_F^2}(1-\kappa), \tag{1}$$

where m is the ^{6}Li mass. Here, z_F^2 is defined by $3m\omega_z^2 z_F^2 \equiv E_F$, and is weakly dependent on the magnetic field through the trap frequencies. The correction factor $1-\kappa$ arises from anharmonicity [20] in the shallow trapping potential $U_0 \simeq 10E_F$ used in the experiments. We find that κ varies from 3% at our lowest energies to 13% at the highest. For simplicity, we neglect an approximately 1% correction arising from the finite scattering length at 840 G.

The entropy of the strongly interacting gas at 840 G is determined using an adiabatic sweep of the magnetic field to 1200 G, where the entropy can be estimated from the mean square axial cloud size $\langle z^2\rangle_{1200}$. At 1200 G, the gas is weakly interacting in our shallow trap, since $k_F a_S = -0.75$, where $a_S = -2900$ bohr [19] and $k_F = (2mE_F/\hbar^2)^{1/2}$. We observe ballistic expansion of the cloud at this field, even at our lowest temperatures, which also shows that the gas is normal.

The dependence of the entropy on $\langle z^2\rangle_{1200}$ can be estimated, in the simplest approximation, by assuming a noninteracting Fermi gas in a Gaussian trapping potential [20]. First, the particle spatial density is determined as a function of T/T_F using the occupation number $f(\epsilon)$ for a Fermi gas. Normalization to the atom number then yields the chemical potential. From the spatial density, we determine $\langle z^2\rangle$ as a function of T/T_F. Then, the energy per particle $E_I(T/T_F)$ is obtained by integrating $\epsilon f(\epsilon)$ with the density of states. Finally, the entropy per particle $S_I(T/T_F)$ is obtained by integrating the entropy per orbital, $s = -k_B[f\ln f + (1-f)\ln(1-f)]$. Together, these results yield $S_I(\langle z^2\rangle)$ as well as $S_I(E_I)$.

We find that the calculated ideal gas $S_I(\langle z^2\rangle)$ differs from a many-body prediction at $k_F a_S = -0.75$ [21] by less than 1% over the range of energies we studied, except at the point of lowest measured energy, where they differ by 10%. For this comparison, we slightly shift the ground state size of the ideal gas to coincide with that calculated for $k_F a_S = -0.75$. Hence, at 1200 G, the shape of the entropy versus cloud size curve is nearly identical to that for an ideal gas. Measurements of $\langle z^2\rangle_{1200}$ therefore provide an essentially model-independent estimate of the entropy of the strongly interacting gas.

Ideally, a sweep from 840 G to a magnetic field of 528 G, where the scattering length vanishes, would produce a noninteracting gas ($k_F a_S = 0$), where the entropy is precisely known. Unfortunately, adiabatic formation of molecules [22] and subsequent molecular decay at fields below resonance [10] cause unwanted heating for such a downward sweep.

To measure the entropy as a function of energy, we start with an energy near the ground state and controllably increase the energy of the gas by releasing the cloud for an adjustable time and then recapturing it, as described previously [5]. After recapture, the gas is allowed to reach equilibrium for 0.7 s. This thermalization time is omitted for the measurement of the ground state size, where no energy is added.

After equilibrium is established, the magnetic field is either ramped to 1200 G over a period of 1 s, or the gas is held at 840 G for 1 s. In either case, after 1 s, the gas is released from the optical trap for a short time to increase the transverse dimension of the cloud for imaging, without significantly changing (less than 0.5%) the measured axial cloud sizes that determine S and E, respectively.

We find that the magnetic field sweep is nearly adiabatic, since the mean square size of the cloud at 840 G after a round-trip sweep of 2 s duration is found to be within 3% of that obtained after a hold time of 2 s at 840 G. However, we also find for our shallow trap that there is a magnetic field and energy independent heating rate, which causes the mean square size to slowly increase at a rate of $\dot{\langle z\rangle^2} = 0.024 z_F^2/s$, corresponding to 24 nK/s in energy units. Since we desire the energy and entropy just after equilibration, we subtract $\dot{\langle z\rangle^2} \times 1$ s from the measured mean square axial dimensions for both the 840 G and 1200 G data. The maximum correction is 5% at the lowest energies.

Figure 1 shows the ratio of the mean square axial cloud size at 1200 G (measured after the sweep) to that at 840 G (measured without the sweep), as a function of the energy of the strongly interacting gas at 840 G. The energy at 840 G is directly measured from the axial cloud size at 840 G using Eq. (1). The displayed ratio and energy scale are independent of the atom number and trap parameters. This is accomplished by measuring the mean square sizes at each field in units of z_F^2 for the given field and atom number. The total data comprise 900 measurements which have been averaged in energy bins of width $\Delta E = 0.04 E_F$.

We note that potential energy has been measured previously in ^{40}K [23] at a Feshbach resonance and after an adiabatic sweep to the noninteracting regime. In Ref. [23], the resulting potential energy ratios are given as a function of the temperature of the noninteracting gas. In contrast, by exploiting universality, our cloud size ratios are referred to the total energy in the strongly interacting regime, which enables a measurement of $S(E)$ and T for the strongly interacting gas.

For our measurements of S at 1200 G, we must have $S = 0$ when $\langle z^2\rangle_{1200}$ attains the ground state value $\langle z^2\rangle_0 = \sigma^2/8$, where σ is the Fermi radius. We determine σ and T/T_F by fitting the spatial profiles at the lowest temperatures with a Sommerfeld approximation for the density

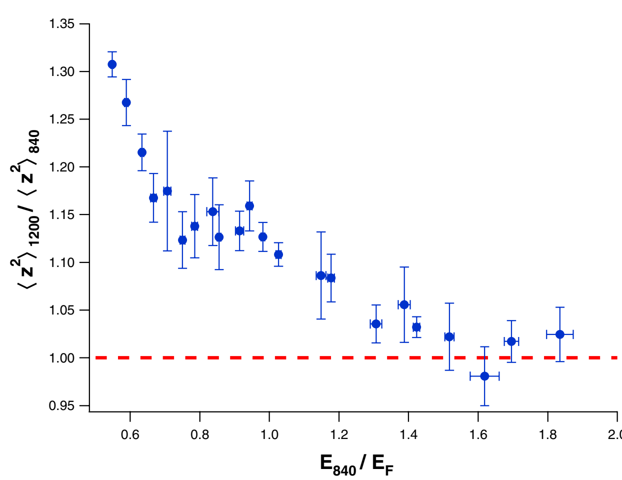

FIG. 1 (color online). Ratio of the mean square cloud size at 1200 G, $\langle z^2\rangle_{1200}$, to that at 840 G, $\langle z^2\rangle_{840}$, for an isentropic magnetic field sweep. E_{840} is the total energy per particle of the strongly interacting gas at 840 G and E_F is the ideal gas Fermi energy. The ratio converges to unity at high energy, as expected (dashed red line).

[24]. We obtain $\langle z^2\rangle_0/z_F^2 = 0.71(0.02)$. For comparison, we can predict the ground state cloud size at 1200 G using the equation of state at zero temperature for the chemical potential versus local density, $\mu(n)$. For negative scattering lengths, using Ref. [25], we find $n(\mu)$. Then, using $\mu = \mu_g - U$, we determine the density for a Gaussian potential U to include anharmonicity. Normalization to the number of atoms yields the global chemical potential μ_g and the mean square cloud size. At 1200 G, where $k_F a_S = -0.75$, we find $\langle z^2\rangle_0/z_F^2 = 0.69$, in good agreement with our measurements.

To convert the data of Fig. 1 into an entropy measurement, we calculate the entropy at 1200 G in the form $S[(\langle z^2\rangle_{1200} - \langle z^2\rangle_0)/z_F^2]$, using the ideal gas approximation as described above. This method automatically assures that $S = 0$ corresponds to the measured ground state $\langle z^2\rangle_0$ at 1200 G, and compensates for the mean field shift between the measured $\langle z^2\rangle_0$ and that calculated for an ideal gas in our Gaussian trapping potential, $0.77z_F^2$.

Figure 2 shows the entropy (blue dots) of the strongly interacting gas at 840 G as a function of its energy in the range $0.4 \le E_{840}/E_F \le 2.0$. The maximum energy is restricted to avoid evaporation in our shallow trap, which can reduce the energy and the atom number during the time of the magnetic field sweep. The entropy of the strongly interacting gas differs significantly from that of an ideal gas (lower orange dot-dashed line), which has a larger ground state energy $E_{I0} = 0.75E_F$. In addition, the data are compared to predictions in the resonant regime based on pseudogap theory [21,26] (dashed green line) and quantum Monte Carlo methods (dotted red line) [27,28].

The temperature is determined in a model-independent manner from $1/T = \partial S(E)/\partial E$. This requires parametrizing the $S(E)$ data to obtain a smooth curve. The simplest assumption consistent with $S(E = E_0) = 0$ is to approximate the data by a power law in $E - E_0$, where E_0 is the ground state energy. To allow for the different scaling of S and E with temperature above and below the superfluid transition [5,26], we use the simple form,

$$S_<(E) = k_B a\left(\frac{E - E_0}{E_F}\right)^b; \qquad E_0 \le E \le E_c$$
$$S_>(E) = S_<(E_c)\left(\frac{E - E_0}{E_c - E_0}\right)^d; \qquad E \ge E_c, \tag{2}$$

where the fit parameters are a, b, d, and E_c. We find that a good fit is obtained using these two different power laws, one above and one below a critical energy E_c. The fit yields a χ^2 per degree of freedom $\simeq 1$, a factor of 2 smaller than that obtained by fitting a single power law to all of the data. We find that Eq. (2) also provides a very close parametrization of the theoretical curves shown in Fig. 2. However, Eq. (2) ignores the smooth transition in slope near E_c, as required for continuity of the temperature, since the detailed critical behavior near E_c is not resolvable in our data. For the power law fits, we take $E_0 \simeq E_{\min} = 0.53(0.02)E_F$, the minimum measured energy, which is close to the estimated ground state energy, $0.50E_F$, for a unitary gas in a harmonic trap [5,29,30].

Fitting the data of Fig. 2 with Eq. (2), the critical energy is found to be $E_c/E_F = 0.94 \pm 0.05$, with a corresponding critical entropy per particle $S_c = 2.7(\pm 0.2)k_B$. Below E_c, the entropy varies with energy as $S_<(E) = k_B(4.5 \pm 0.2)[(E - E_0)/E_F]^{0.59\pm0.03}$. Above E_c, we obtain $S_>(E) = k_B(4.0 \pm 0.2)[(E - E_0)/E_F]^{0.45\pm0.01}$. We find that the variances of a and b have a positive correlation, so that $S(E)$ is determined more precisely than the independent variation of a and b would imply. The change in behavior near E_c is shown clearly in the inset of Fig. 2.

The power law exponent below E_c, $b = 0.59$, falls between that of an ideal harmonically trapped Fermi gas, where a Sommerfeld expansion at low energy yields $S \propto (E - E_0)^{1/2}$ and that of an ideal harmonically trapped Bose-Einstein condensate, where $S \propto (E - E_0)^{3/4}$. By contrast, above E_c, the exponent $d = 0.45$ is close to the result we obtain by fitting a power law to the calculated entropy of an ideal gas in our Gaussian trap, i.e., $S_I(E - E_{I0}) \propto (E - E_{I0})^q$, with $q = 0.485$ for E below $0.94E_F$ and $q = 0.452$ above. This is a consequence of the cloud size ratios shown in Fig. 1, which converge to unity at higher energies.

The energy versus temperature $E(T)$ is determined from the derivative of the fit function $S(E)$. For $E \le E_c$,

$$\frac{E - E_0}{E_F} = \left(\frac{abT}{T_F}\right)^{1/(1-b)}. \tag{3}$$

From the best fit to the entropy data, where $a = 4.5$, $b = 0.59$, $E_c = 0.94E_F$, we obtain $(E - E_0)/E_F = 11(T/T_F)^{2.44}$ below E_c.

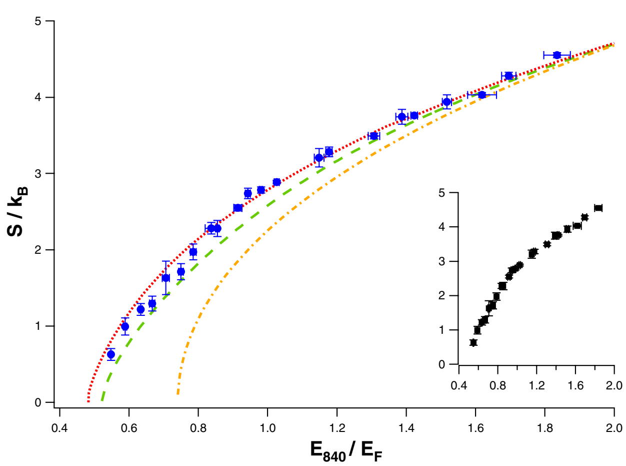

FIG. 2 (color online). Measured entropy per particle of a strongly interacting Fermi gas at 840 G vs its total energy per particle (blue dots). Lower orange dot-dashed curve—ideal gas entropy $S_I(E_I)$; green dashes—pseudogap theory [21]; red dots—quantum Monte Carlo prediction [27]. Inset—entropy vs energy data showing a change in behavior at $E_c = 0.94E_F$.

We estimate the critical temperature T_c using the measured value of $E_c = (0.94 \pm 0.05)E_F$. Here, we interpret E_c as the critical energy for the superfluid transition. This value is consistent with our previous measurements based on the heat capacity, where we observe a change in behavior at $E = 0.85E_F$ [5], and in collective mode damping [17], where a plot of the damping rate versus energy (rather than empirical temperature) shows a change in behavior near $E = 1.01E_F$.

Ideally, to obtain T_c, the fit $S(E)$ should have a continuous slope near E_c. Since our fit function has different slopes above and below E_c, we use the average of the two slopes to approximate the slope of the tangent to a smooth curve through the data at E_c. Inverting Eq. (3) yields $T/T_F = 0.38[(E - E_0)/E_F]^{0.41}$ and $T_{c<}/T_F = 0.26$. Similarly, for $E(T) > E_c$, we find $T/T_F = 0.56[(E - E_0)/E_F]^{0.55}$ and $T_{c>}/T_F = 0.34$. Taking $2/T_c \simeq 1/T_{c<} + 1/T_{c>}$, we find $T_c/T_F = 0.29(+0.03/-0.02)$. Here, the error estimate includes the cross correlations in the variances of a, b, E_c, and d.

The measured critical temperature $T_c/T_F = 0.29(+0.03/-0.02)$ can be compared to our previous estimate of $T_c/T_F = 0.27$ from an experiment with a model dependent temperature calibration [5]. Moreover, the result 0.29 is in good agreement with predictions for trapped atoms, 0.29 [5], 0.30 [31], 0.31 [30], 0.30 [32], 0.26 [6], and 0.27 [27,28].

We thank Ingrid Kaldre for help in constructing the cold atom source. We are grateful to Qijin Chen and Kathy Levin, U. Chicago, and Aurel Bulgac and Joaquín E. Drut, U. Washington, Seattle, for providing calculations of the entropy versus cloud size in advance of publication. We also thank Jason Ho for many discussions about entropy and energy measurement, which stimulated this work. This research is supported by the Chemical Sciences, Geosciences, and Biosciences Division of the Office of Basic Energy Sciences, Office of Science, US Department of Energy, the Physics Divisions of the Army Research Office and the National Science Foundation, and the Physics for Exploration program of the National Aeronautics and Space Administration.

*Email address: jet@phy.duke.edu

[1] K. M. O'Hara, S. L. Hemmer, M. E. Gehm, S. R. Granade, and J. E. Thomas, Science **298**, 2179 (2002).
[2] H. Heiselberg, Phys. Rev. A **63**, 043606 (2001).
[3] T.-L. Ho, Phys. Rev. Lett. **92**, 090402 (2004).
[4] J. E. Thomas, A. Turlapov, and J. Kinast, Phys. Rev. Lett. **95**, 120402 (2005).
[5] J. Kinast, A. Turlapov, J. E. Thomas, Q. Chen, J. Stajic, and K. Levin, Science **307**, 1296 (2005).
[6] H. Hu, X.-J. Liu, and P. D. Drummond, Phys. Rev. A **73**, 023617 (2006).
[7] C. A. Regal, M. Greiner, and D. S. Jin, Phys. Rev. Lett. **92**, 040403 (2004).
[8] M. W. Zwierlein, C. A. Stan, C. H. Schunck, S. M. F. Raupach, A. J. Kerman, and W. Ketterle, Phys. Rev. Lett. **92**, 120403 (2004).
[9] J. Kinast, S. L. Hemmer, M. E. Gehm, A. Turlapov, and J. E. Thomas, Phys. Rev. Lett. **92**, 150402 (2004).
[10] T. Bourdel, L. Khaykovich, J. Cubizolles, J. Zhang, F. Chevy, M. Teichmann, L. Tarruell, S. Kokkelmans, and C. Salomon, Phys. Rev. Lett. **93**, 050401 (2004).
[11] C. Chin, M. Bartenstein, A. Altmeyer, S. Riedl, S. Jochim, J. H. Denschlag, and R. Grimm, Science **305**, 1128 (2004).
[12] G. B. Partridge, K. E. Strecker, R. I. Kamar, M. W. Jack, and R. G. Hulet, Phys. Rev. Lett. **95**, 020404 (2005).
[13] C. A. R. Sá de Melo, M. Randeria, and J. R. Engelbrecht, Phys. Rev. Lett. **71**, 3202 (1993).
[14] M. Holland, S. J. J. M. F. Kokkelmans, M. L. Chiofalo, and R. Walser, Phys. Rev. Lett. **87**, 120406 (2001).
[15] E. Timmermans, K. Furuya, P. W. Milonni, and A. K. Kerman, Phys. Lett. A **285**, 228 (2001).
[16] Q. Chen, J. Stajic, S. Tan, and K. Levin, Phys. Rep. **412**, 1 (2005).
[17] J. Kinast, A. Turlapov, and J. E. Thomas, Phys. Rev. Lett. **94**, 170404 (2005).
[18] M. Zwierlein, J. Abo-Shaeer, A. Schirotzek, C. Schunck, and W. Ketterle, Nature (London) **435**, 1047 (2005).
[19] M. Bartenstein *et al.*, Phys. Rev. Lett. **94**, 103201 (2005).
[20] We approximate the trapping potential by $U = U_0\{1 - \exp[-m\bar{\omega}^2 r^2/(2U_0)]\}$. In this case, we find $\kappa = 5m\omega_z^2\langle z^4\rangle/(8U_0\langle z^2\rangle)$. For total energies above E_F, where the spatial distribution is nearly Gaussian, one readily obtains $\langle z^4\rangle = 3\langle z^2\rangle^2$ and $\kappa = (5E_F/8U_0)\langle z^2\rangle/z_F^2$.
[21] Q. Chen, Pseudogap Theory, trapped Fermi gas at a Feshbach resonance (private communication). For the resonant case, $1/(k_F a) = 0.11$ is used [5].
[22] C. A. Regal, C. Ticknor, J. L. Bohn, and D. S. Jin, Nature (London) **424**, 47 (2003).
[23] J. T. Stewart, J. P. Gaebler, C. A. Regal, and D. S. Jin, Phys. Rev. Lett. **97**, 220406 (2006).
[24] M. E. Gehm, S. L. Hemmer, S. R. Granade, K. M. O'Hara, and J. E. Thomas, Phys. Rev. A **68**, 011401(R) (2003).
[25] C. Chin, Phys. Rev. A **72**, 041601(R) (2005).
[26] Q. Chen, J. Stajic, and K. Levin, Phys. Rev. Lett. **95**, 260405 (2005).
[27] A. Bulgac, Quantum Monte Carlo Theory, trapped Fermi gas at a Feshbach resonance (private communication).
[28] A. Bulgac, J. E. Drut, and P. Magierski, Phys. Rev. Lett. **96**, 090404 (2006).
[29] J. Carlson, S.-Y. Chang, V. R. Pandharipande, and K. E. Schmidt, Phys. Rev. Lett. **91**, 050401 (2003).
[30] A. Perali, P. Pieri, and G. C. Strinati, Phys. Rev. Lett. **93**, 100404 (2004).
[31] J. Kinnunen, M. Rodríguez, and P. Törmä, Science **305**, 1131 (2004).
[32] P. Massignan, G. M. Bruun, and H. Smith, Phys. Rev. A **71**, 033607 (2005).